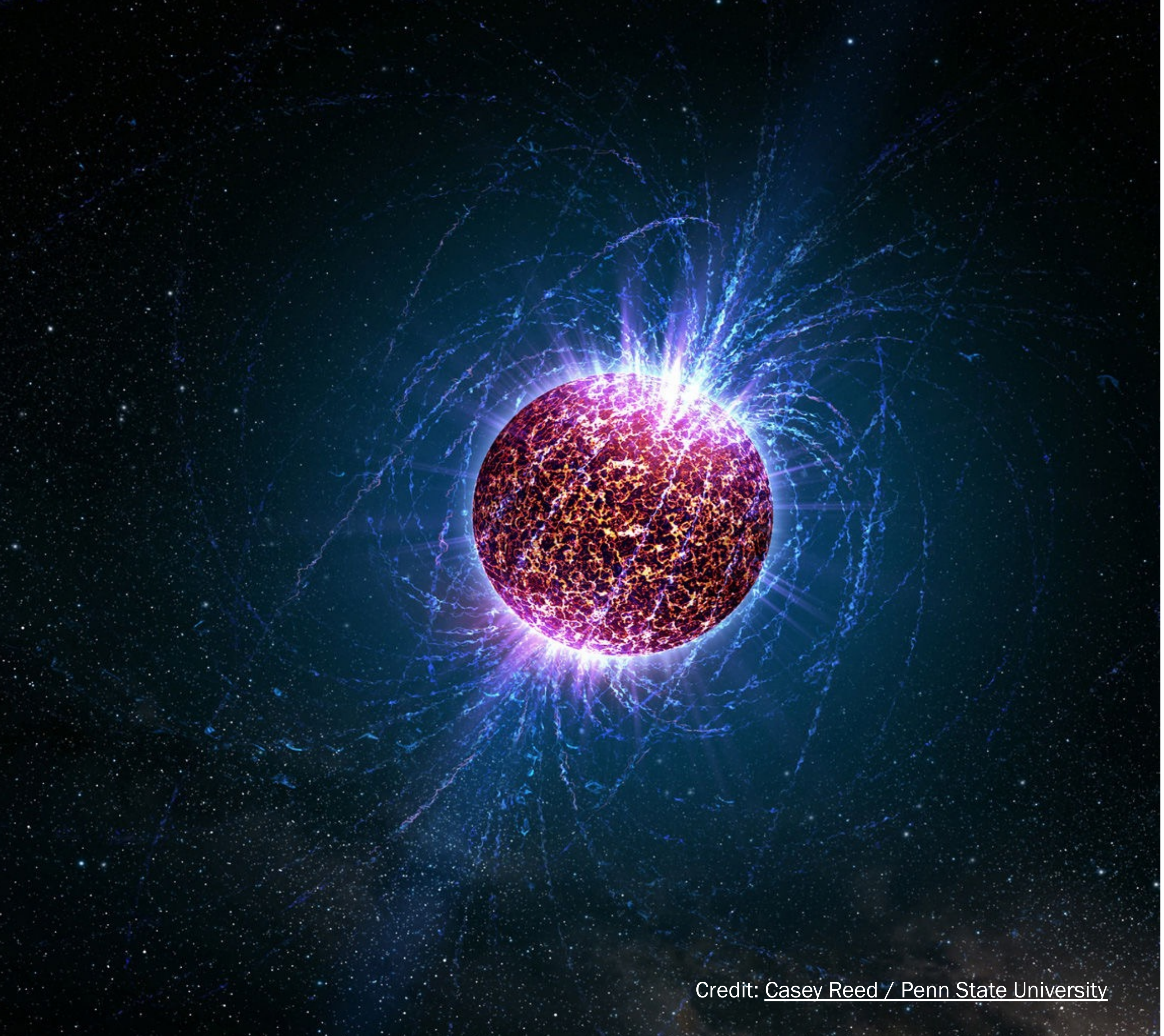
Credit: Casey Reed / Penn State University

ANISOTROPIC HYBRID STARS

Interplay of superconductivity and magnetic field leading to gravitational waves

arXiv: 2604.06308

Zenia Zuraiq
Indian Institute of Science
Work done with
Banibrata Mukhopadhyay (IISc)

INDIAN INSTITUTE OF SCIENCE
भारतीय विज्ञान संस्थान

6th Zeldovich Meeting
Pescara, Italy
14/07/2026

How heavy can a NS get?

We have shown that massive neutron stars, with structure effects from magnetic field and anisotropy can explain mass gap objects ($> 2.5M_{\odot}$), satisfying stability and observational constraints.
ZZ, Mukhopadhyay, Weber, Phys. Rev. D. (2024)

Adding more physics!
Superconductivity,
Deconfined quarks

arXiv: 2604.06308

QUARK/STRANGE/HYBRID STARS

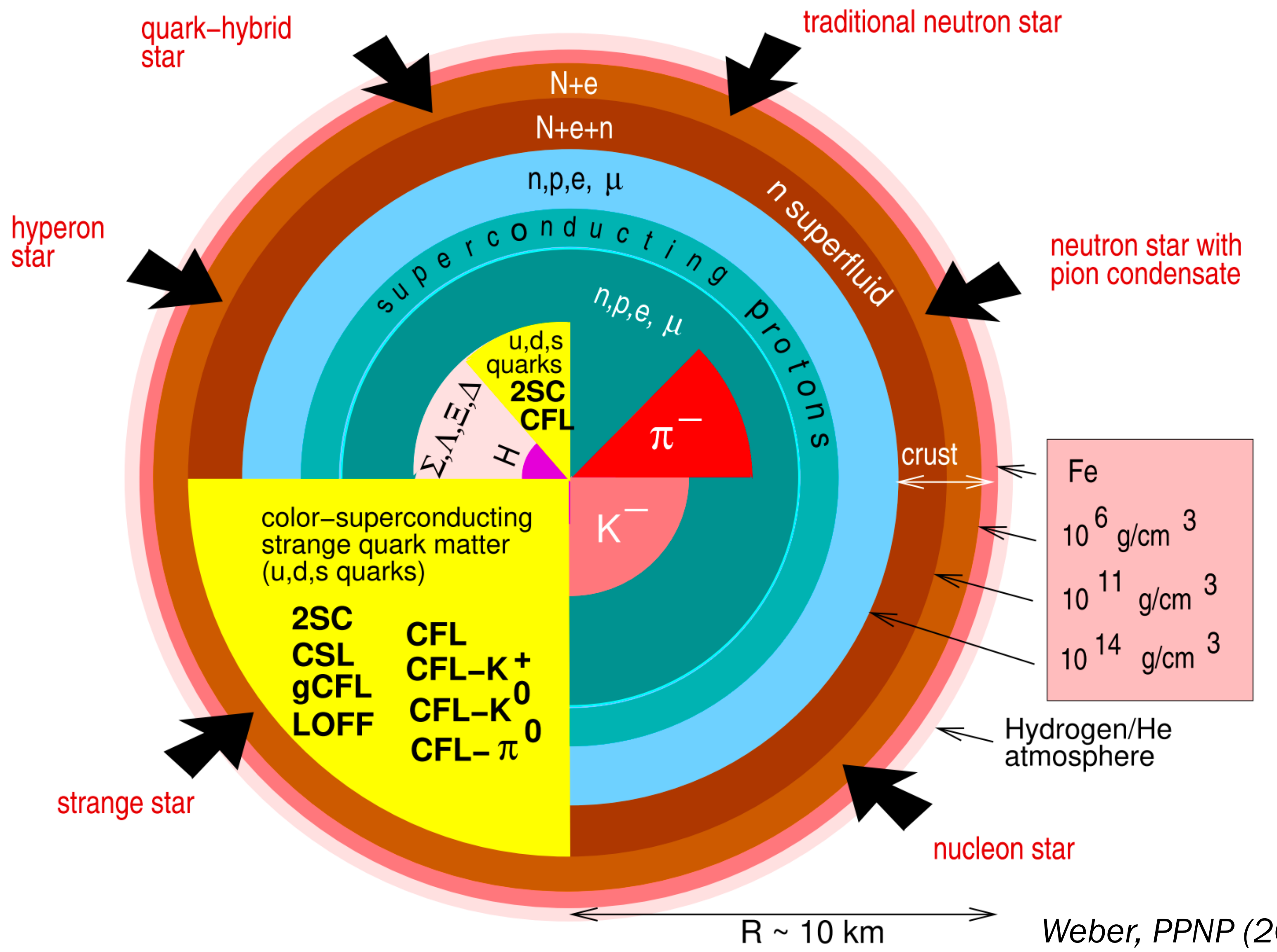

Weber, PPNP (2005)

COLOR SUPERCONDUCTIVITY

Weber, PPNP (2005)

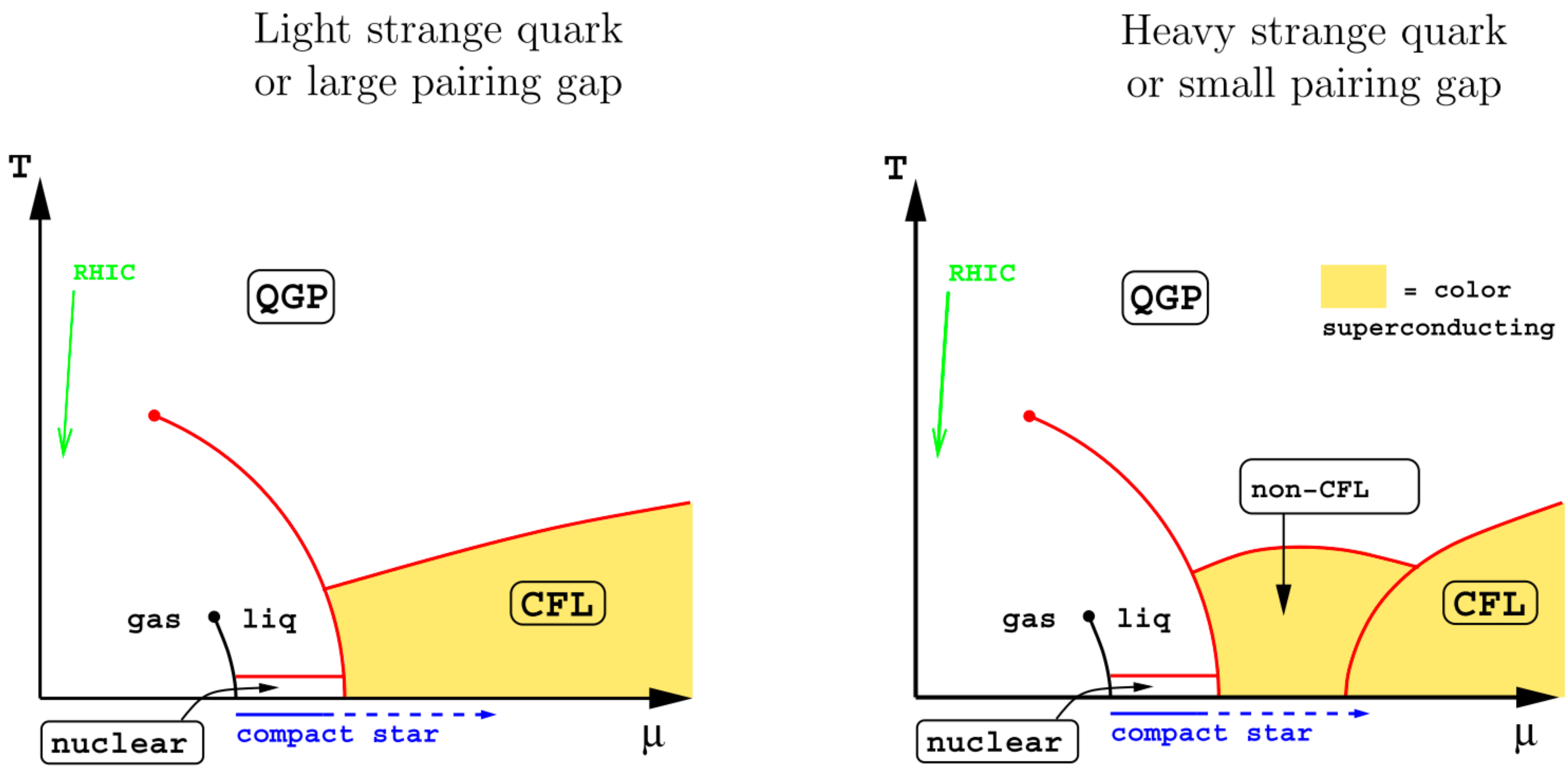

CFL → Color-flavor locked state → u,d,s quarks pair

Non-CFL → 2SC, CSL, etc.

Δ_{SC} = 10 -100 MeV

Pairing gaps higher than proton case

→ higher critical fields required to destroy color superconductivity

Color superconducting (CSC) matter → source of deformation/anisotropy?

High field cases: $B_s = 10^{15}\ G, B_0 = 10^{18}\ G$

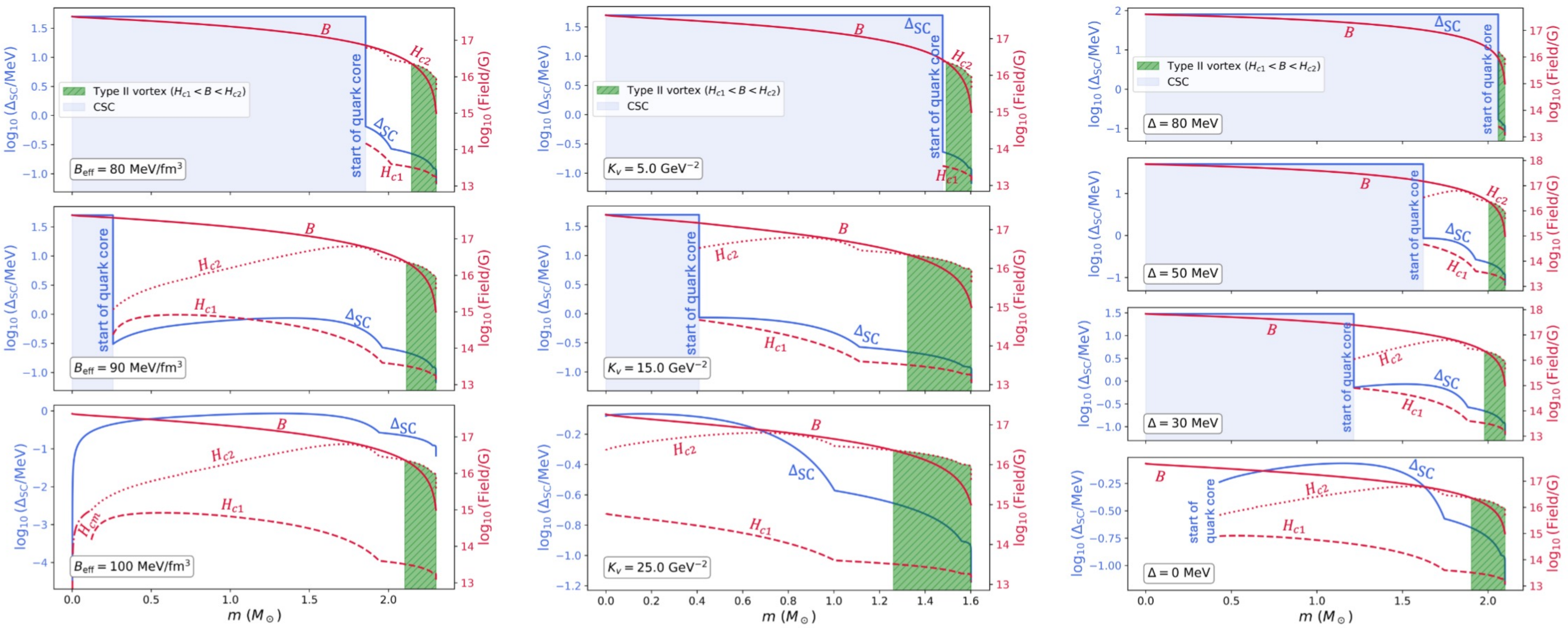

Magnetar cores are not devoid of superconductivity!

Only **proton** superconductivity is destroyed

→ **Color superconductivity can still persist**

HYBRID STAR EQUATION OF STATE (EoS)

Hadronic EoS: DD2

DDRMF EoS

Typel et al., PRC (2010)

Quark EoS: vBag

Bag model (B_{eff}) + Repulsive vector interactions (K_v)

Klähn & Fischer, ApJ (2015)

Hadronic and quark phases: Joined by sharp first-order phase transition (PT)

→ Maxwell construction

CSC effects included through CSC pairing energy $\Delta_{\mathrm{SC}}^2\mu^2$ in the thermodynamic potential

→ $\Omega_{\mathrm{CFL}} = \Omega_{\mathrm{unpaired}} - (3/\pi^2)\Delta_{\mathrm{SC}}^2\mu^2$ (CFL)

Lugones & Horvath, PRD (2002)

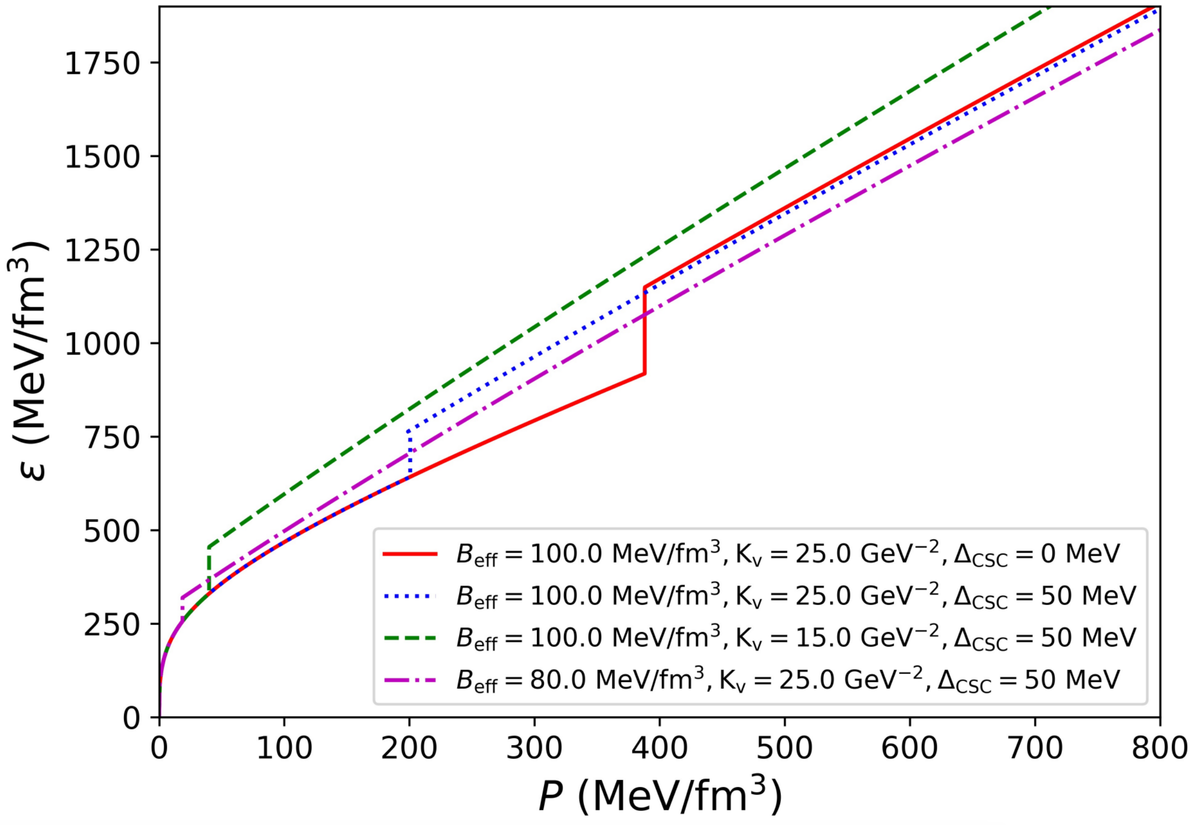

We assume entire quark core is CFL color superconducting with a constant gap Δ_{CSC}

Quark parameters: B_{eff}, K_v and Δ_{CSC} → Determine extent of (color superconducting) quark core

FORMALISM

Modified TOV equations

$$\frac{dm}{dr} = 4\pi r^2 \left(\rho + \frac{B^2}{8\pi}\right)$$

$$\frac{dp_r}{dr} = \begin{cases} \dfrac{\dfrac{-(\rho + p_r)\left[4\pi r^3 \left(p_r - \frac{B^2}{8\pi}\right) + m\right]}{r(r-2m)} + \dfrac{2}{r}\sigma_{\text{aniso}}}{\left[1 - \dfrac{d}{d\rho}\left(\dfrac{B^2}{8\pi}\right)\left(\dfrac{d\rho}{dp_r}\right)\right]} & \text{For radially oriented (RO) fields} \\[2em] \dfrac{\dfrac{-\left(\rho + p_r + \frac{B^2}{4\pi}\right)\left[4\pi r^3 \left(p_r + \frac{B^2}{8\pi}\right) + m\right]}{r(r-2m)} + \dfrac{2}{r}\sigma_{\text{aniso}}}{\left[1 + \dfrac{d}{d\rho}\left(\dfrac{B^2}{8\pi}\right)\left(\dfrac{d\rho}{dp_r}\right)\right]} & \text{For transversely oriented (TO) fields} \end{cases}$$

Deb, Mukhopadhyay & Weber, ApJ (2021, 2022)

ZZ, Mukhopadhyay, Weber, Phys. Rev. D (2024)

Ansatz for anisotropy

Magnetic Field profile used

$$B(P) = B_s + B_0 \left[1 - \exp\left\{-\eta \left(\frac{P}{P_0}\right)^{\gamma}\right\}\right]$$

ZZ et al., Universe (2026)

Bandyopadhyay et al. , PRL (1997)

ANISOTROPY PROFILES

(color/proton) Superconductivity + Magnetic field = Anisotropy

Profile 1: Multiplicative

Role of (color/proton) Superconductivity → Enhancing magnetic stresses in star

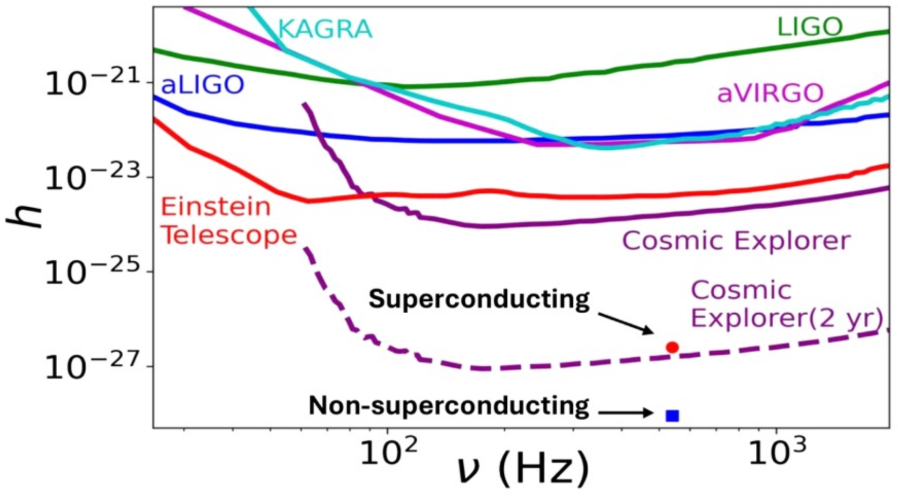

Das, Sedrakian, Mukhopadhyay, PRD Lett., (2025)

$$\sigma_{\text{aniso}} = p_t - p_r = \left(\frac{2m}{r}\right)(\pm B^2)\left(1 + \frac{\Delta_{\text{SC}}^2 \mu^2}{p_r}\right)\left(\frac{p_r}{p_c}\right)$$

Following **quasilocal model** of anisotropy; Ensures anisotropy vanishes at center

Magnetic stress anisotropy

Enhancement from superconductivity

Ensures anisotropy vanishes at surface

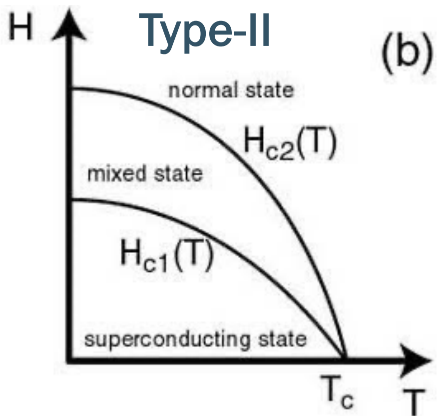

Following behavior of **Type II superconductors** (*Easson & Pethick, PRD, 1977*) and **MCFL phase** (*Paulucci et al., PRD, 2011*)
→ Superconductivity coupled to magnetic field stresses

ANISOTROPY PROFILES

(color/proton) Superconductivity + Magnetic field = Anisotropy

Profile 2: Additive

Role of (color/proton) Superconductivity → Introducing its own anisotropic stress to the star

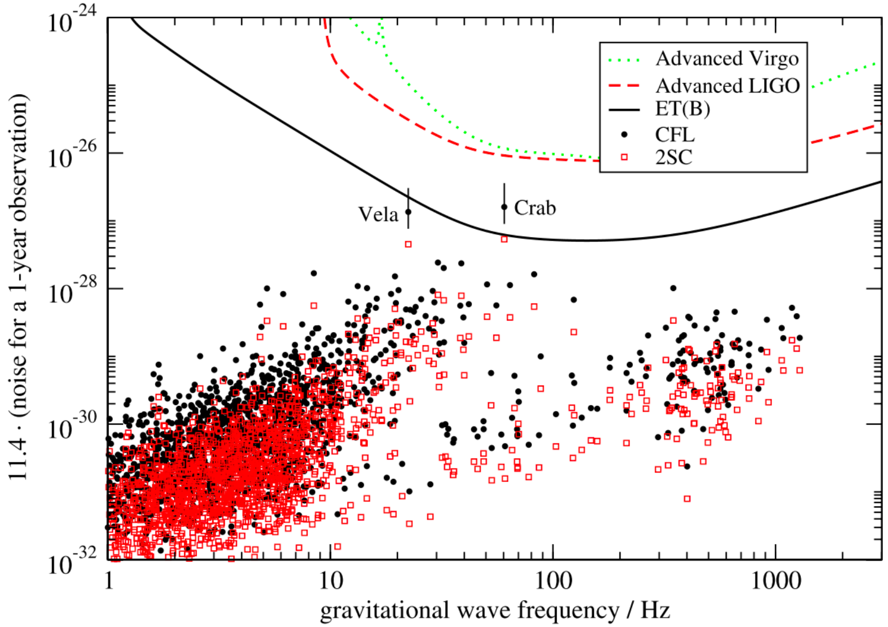

Glampedakis, Jones, Samuelsson, PRL (2012)

$$\sigma_{\text{aniso}} = p_t - p_r = \left(\frac{2m}{r}\right)\left(\pm B^2 + \Delta_{\text{SC}}^2 \mu^2\right)\left(\frac{p_r}{p_c}\right)$$

Following **quasilocal model** of anisotropy; Ensures anisotropy vanishes at center

Magnetic stress anisotropy

Enhancement from superconductivity

Ensures anisotropy vanishes at surface

Following behavior of **Crystalline color superconducting phases** (*Mannarelli, Rajagopal & Sharma, PRD, 2007*)

→ Superconductivity can lead to independent anisotropic stresses

ENHANCED $M_{\max}$

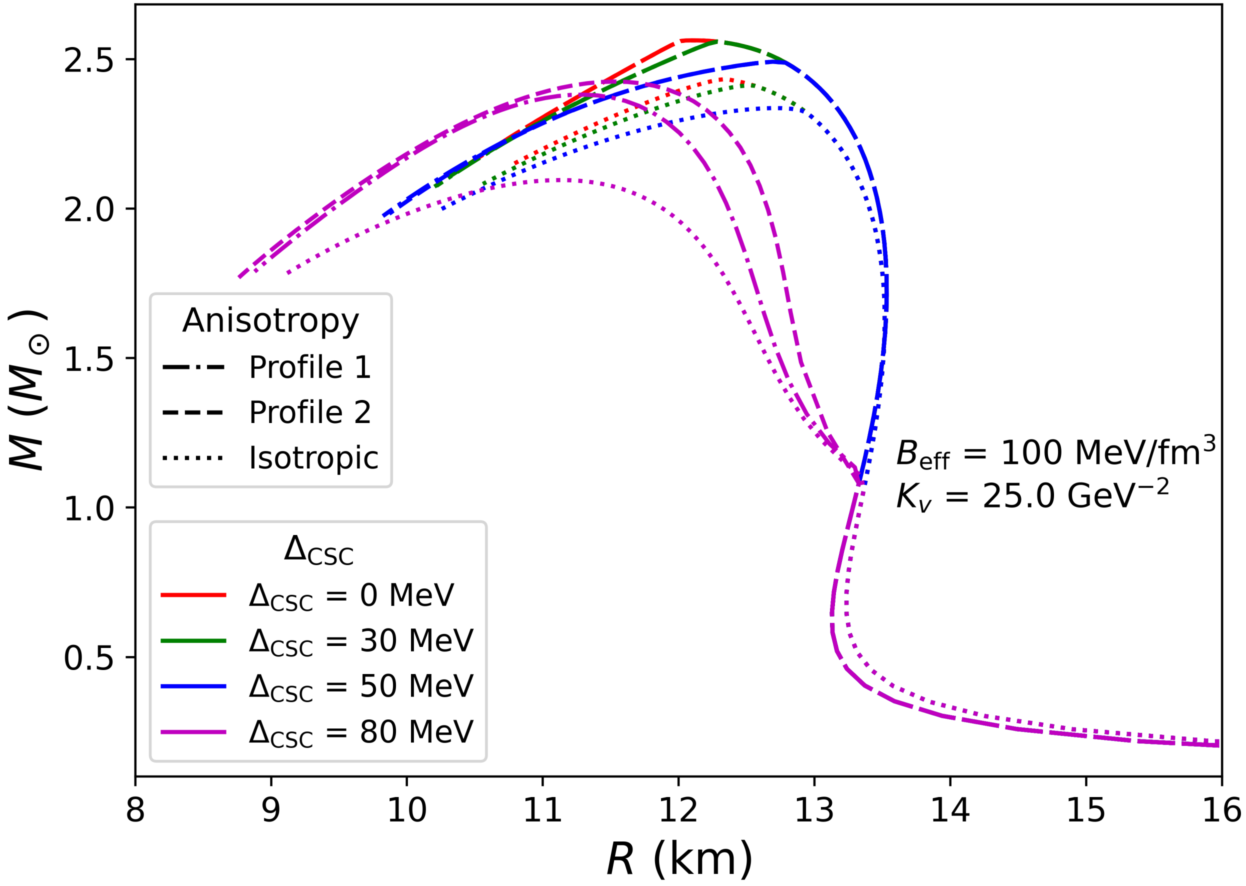

Magnetic field profile:
$\eta = 0.01, \gamma = 1, B_s = 10^{15}\ G, B_0 = 10^{18}\ G$, TO

Presence of CSC quark core leads to **CSC softening**: Compensated by anisotropy for $\Delta_{CSC} > 50$ MeV

In the presence of high fields:
$B_s = 10^{15}\ G, B_0 = 10^{18}\ G$ **(Magnetar)**

- Magnetic fields dominate the anisotropy and/or anisotropy effects
- When the PT leads to unstable branch → Magnetic field enhances mass of hadron star before quark core forms

In the presence of low fields:
$B_s = 10^{12}\ G, B_0 = 10^{15}\ G$ **(Regular NS)**

- Magnetic field effect sub-dominant; cannot enhance mass
- **Profile 2 → shows enhancement of mass for** $\Delta_{CSC} > 50$ MeV; independent of field. Not the case for Profile 1 (Δ_{CSC} coupled to low field)

ENHANCED $M_{\max}$

Presence of CSC quark core leads to **CSC softening**: Compensated by anisotropy for $\Delta_{CSC} > 50$ MeV

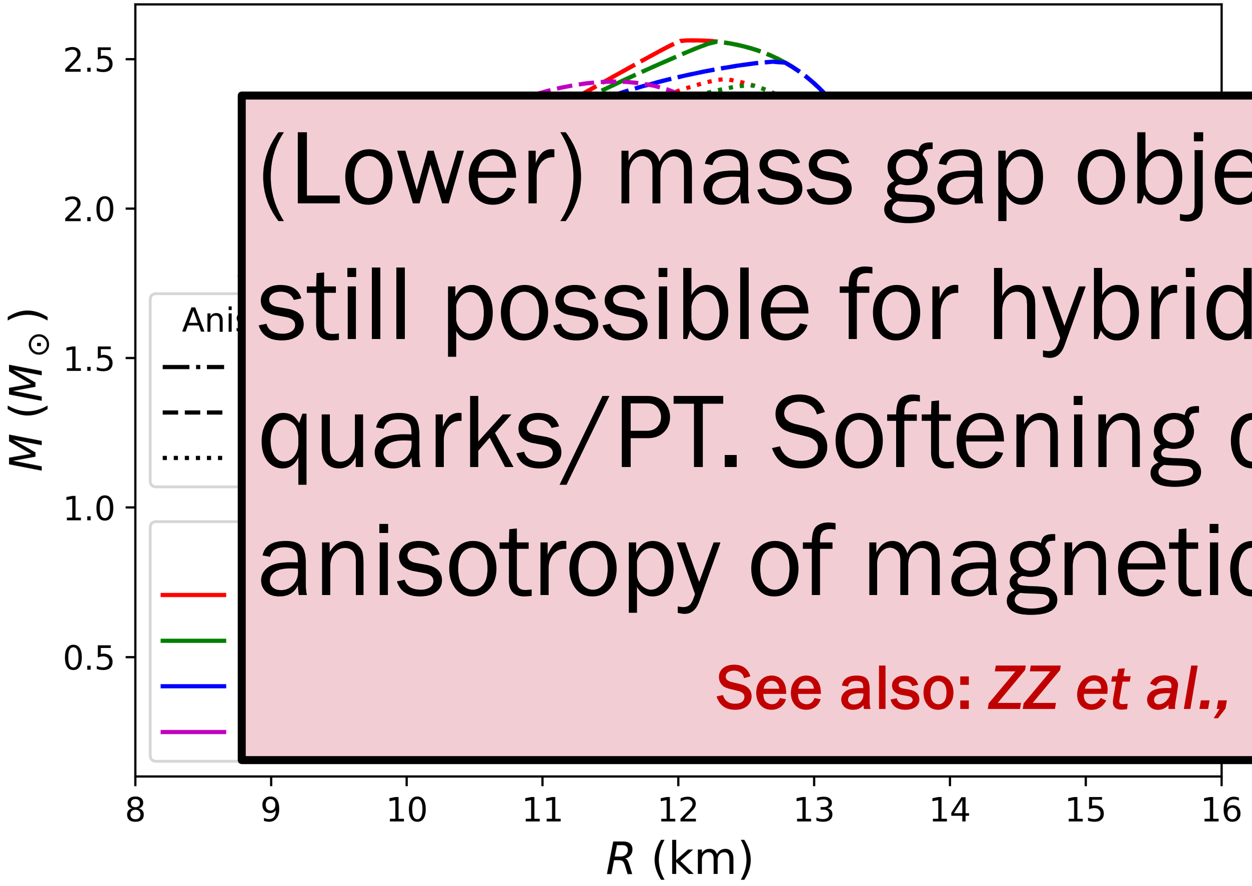

Magnetic field profile:
$\eta = 0.01, \gamma = 1, B_s = 10^{15}\ G, B_0 = 10^{18}\ G$, TO

(Lower) mass gap objects ($\sim 2.5 - 2.6 M_\odot$) still possible for hybrid stars with CSC quarks/PT. Softening compensated by anisotropy of magnetic field/CSC matter.

See also: *ZZ et al., Universe (2026)*

In the presence of high fields:

and/or

star

- Magnetic field effect sub-dominant; cannot enhance mass
- **Profile 2 → shows enhancement of mass for** $\Delta_{CSC} > 50$ MeV; independent of field. Not the case for Profile 1 (Δ_{CSC} coupled to low field)

ANISOTROPY INDUCED DEFORMATION

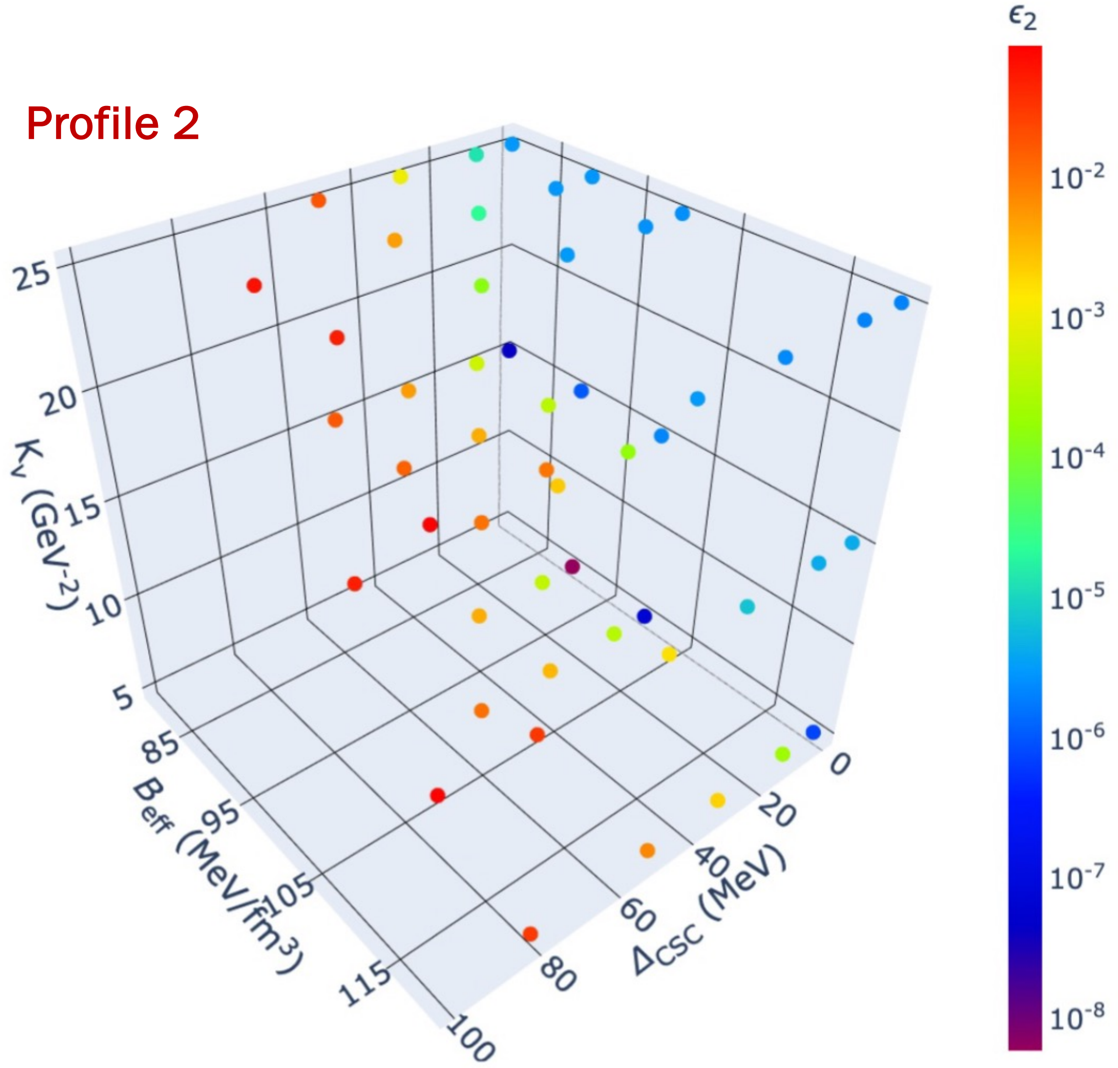

https://zeniazuraiq.github.io/ellipticity_CSCStars

Ellipticity

$$\epsilon = \frac{\pi}{I_0} \int_V dr\, \delta\rho\, r^4$$

Effective 1D treatment: all calculations assume an equatorial slice θ = π/2 in the star

Δ_{CSC}	ϵ_{mag}	ϵ_1	ϵ_2
30 MeV	8.7×10^{-10}	2.4×10^{-9}	3.1×10^{-5}
50 MeV	7.1×10^{-10}	1.8×10^{-9}	2.0×10^{-4}
80 MeV	8.8×10^{-10}	2.7×10^{-8}	5.1×10^{-2}

$B_{\rm eff} = 100\ MeV/fm^3,\ K_v = 25\ GeV^{-2}$

CONTINUOUS GRAVITATIONAL WAVES

Deformed, triaxial, rotating star → emits **continuous gravitational waves (CGWs)**

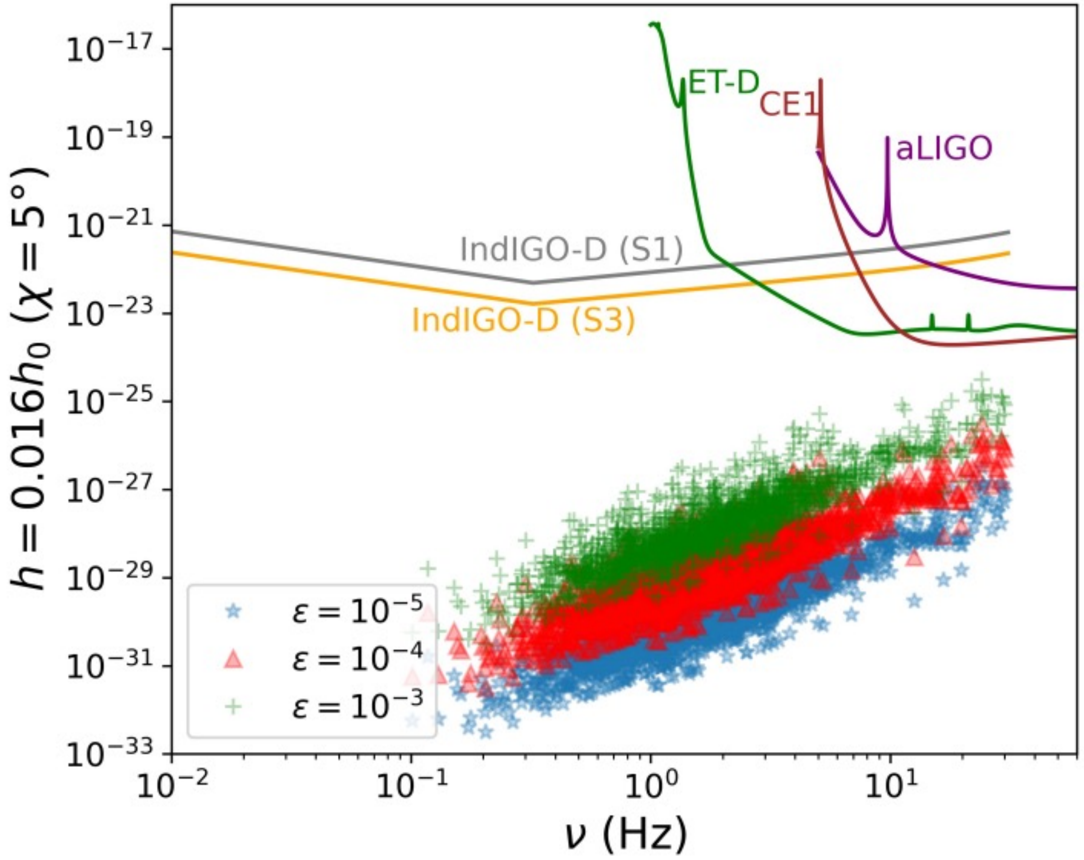

Detection possibility of slow rotating ($\nu < 30\ Hz$) and weakly magnetized ($B_s < 10^{12}\ G$) sources taken from ATNF catalog

For a triaxially deformed star,

$$h_0 = \frac{2G}{c^4} \frac{\Omega^2 \epsilon I_0}{d} (2\cos^2\chi - \sin^2\chi)$$

Kalita & Mukhopadhyay, MNRAS (2019)

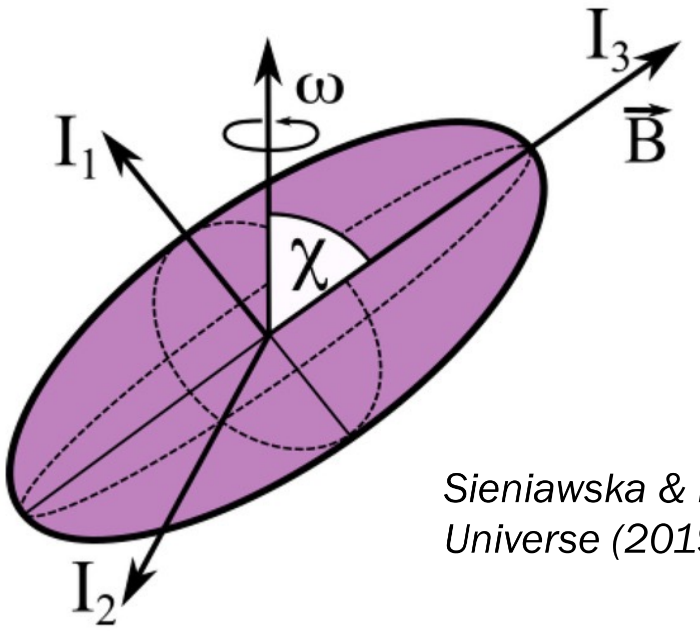

Sieniawska & Bejger, Universe (2019)

CONTINUOUS GRAVITATIONAL WAVES

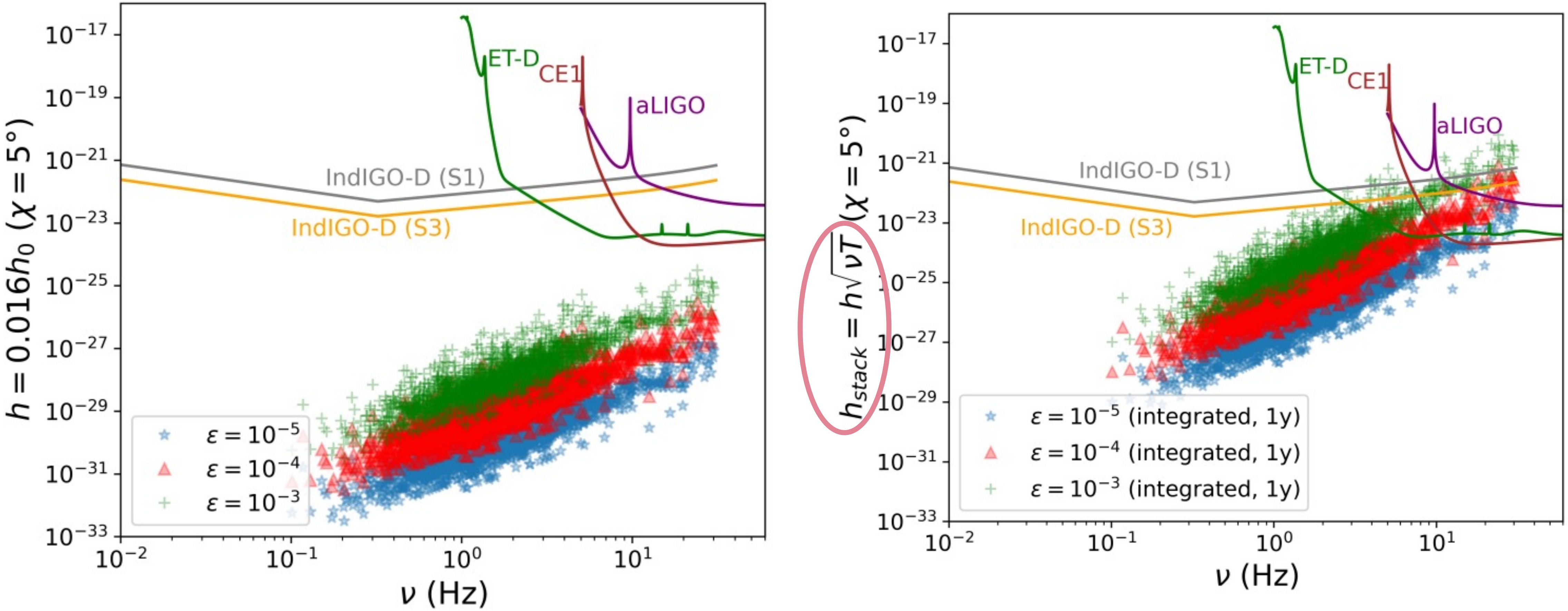

Non-detection from aLIGO → a plausible way to constrain quark properties and/or structural effects of color superconductivity

Maximum detectable distance

$$d_{\max}(\nu,\epsilon) = \frac{2G}{c^4}\frac{\Omega^2 \epsilon I_0}{h_{noise}}\frac{\sqrt{\nu T}}{\mathrm{SNR}_{th}} f(\chi),$$

https://zeniazuraiq.github.io/CGW_ET_CSCStars

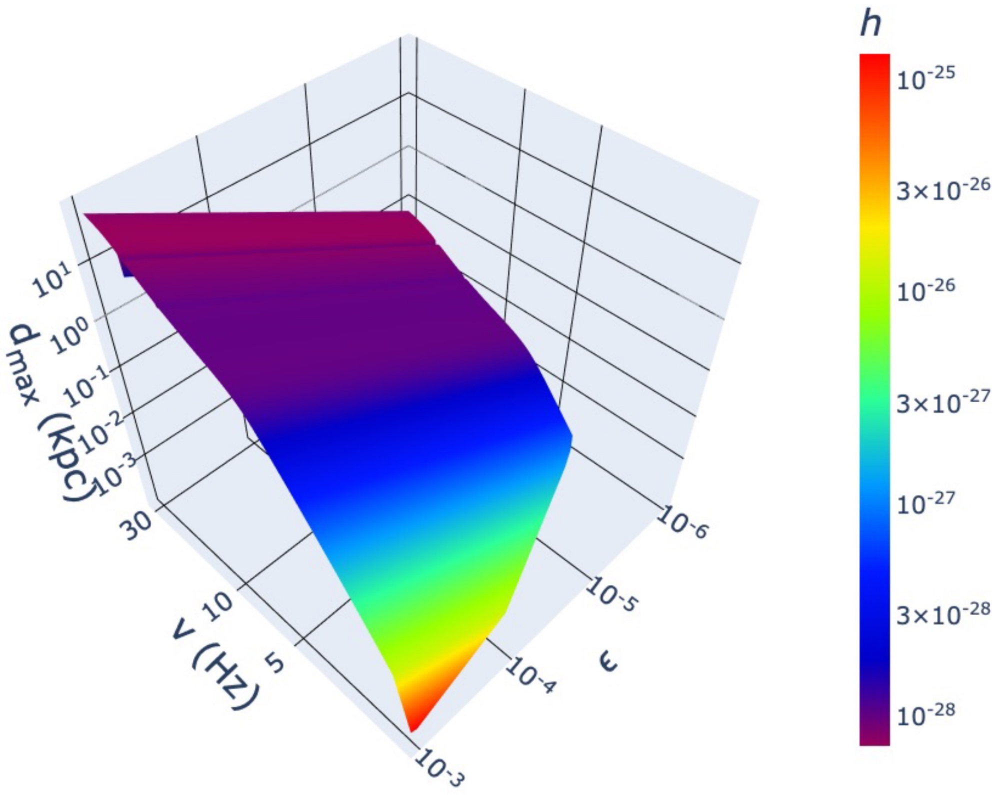

Einstein Telescope

Maximum $d_{\max} = 69$ kpc

> Radius of Milky Way galaxy

https://zeniazuraiq.github.io/CGW_DeciHz_CSCStars

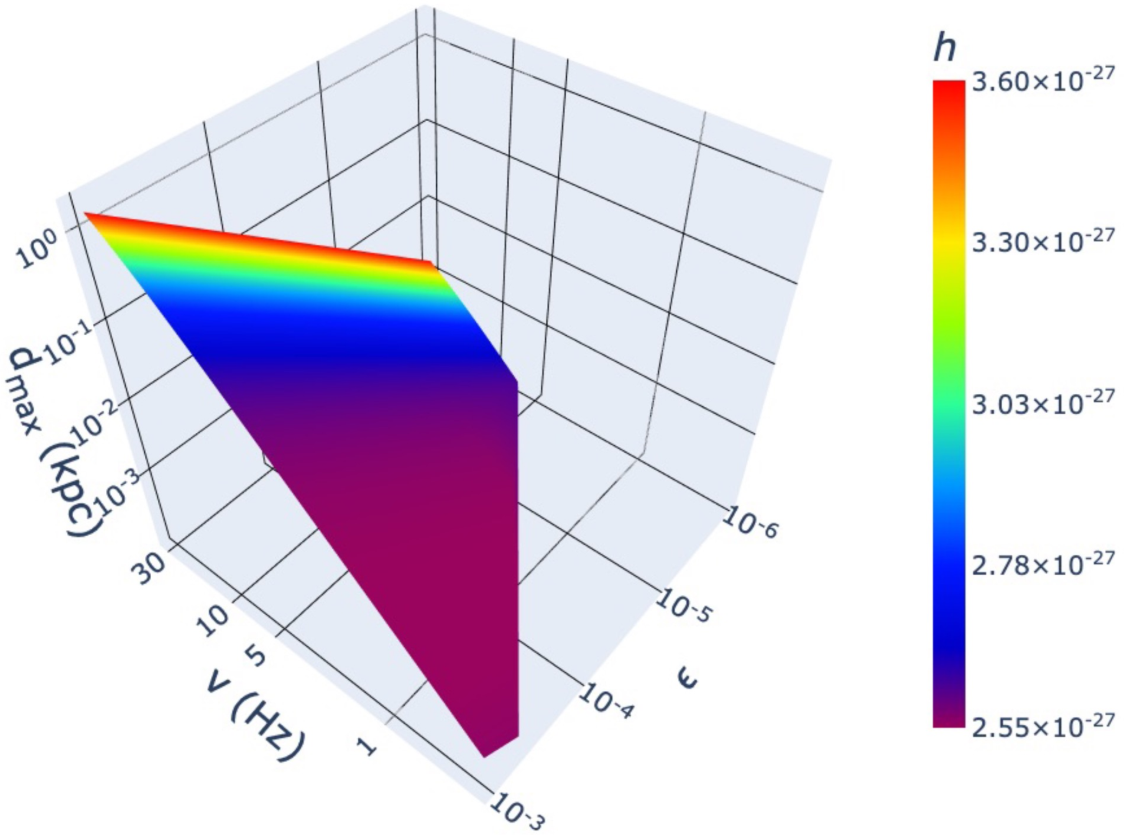

IndIGO-D

Maximum $d_{\max} = 1.5$ kpc

TAKE HOME

Pressure anisotropy in hybrid stars plays a key role in determining its structure, properties and observables.

- Presence of magnetic field and (color/proton) superconductivity → leads to anisotropic stresses in the star.
  We have proposed **two phenomenological profiles** to parameterize anisotropic effects.

- Magnetar/highly magnetized NS cores: NOT devoid of superconductivity.
  Even if proton superconductivity is destroyed, **color superconductivity persists**.

- Anisotropy enhances mass of hybrid stars → overcomes softening effects
  → **Plausibility of mass gap candidates**.

arXiv: 2604.06308

- Enhanced deformation from CSC anisotropic stresses → can make GWs from slow rotating, weakly magnetized NSs observable
  → detection/non-detection **constrains CSC quark core and properties**.

Thank you

PROTON SUPERCONDUCTIVITY

In presence of **type-II** superconducting protons → anisotropic stress gets modified

Easson & Pethick, PRD (1977)

$$\frac{B^2}{8\pi} \rightarrow \frac{BH_{c1}}{8\pi}$$

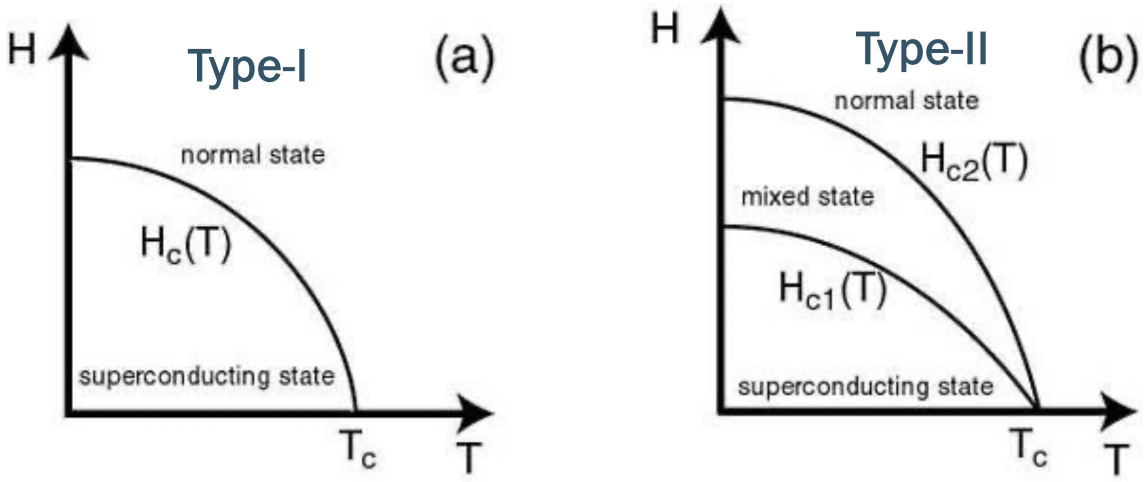

https://uspas.fnal.gov/materials/13Duke/SCL_Chap1.pdf

Proton superconductivity
→ source of deformation/anisotropy?

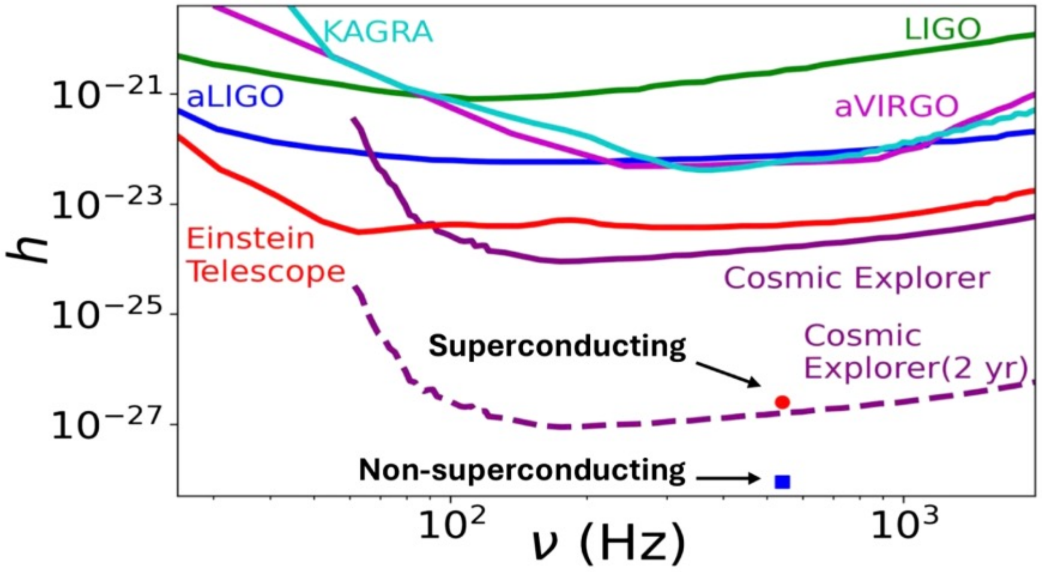

At the cores of magnetars/highly magnetized NSs
→$B > H_{c2}$
→ Proton superconductivity absent

Das, Sedrakian, Mukhopadhyay, PRD Lett., (2025)
Sinha, Sedrakian, Phys. Part. Nucl. (2015)

$$\Delta_{SC} \sim 1 \text{ MeV}$$

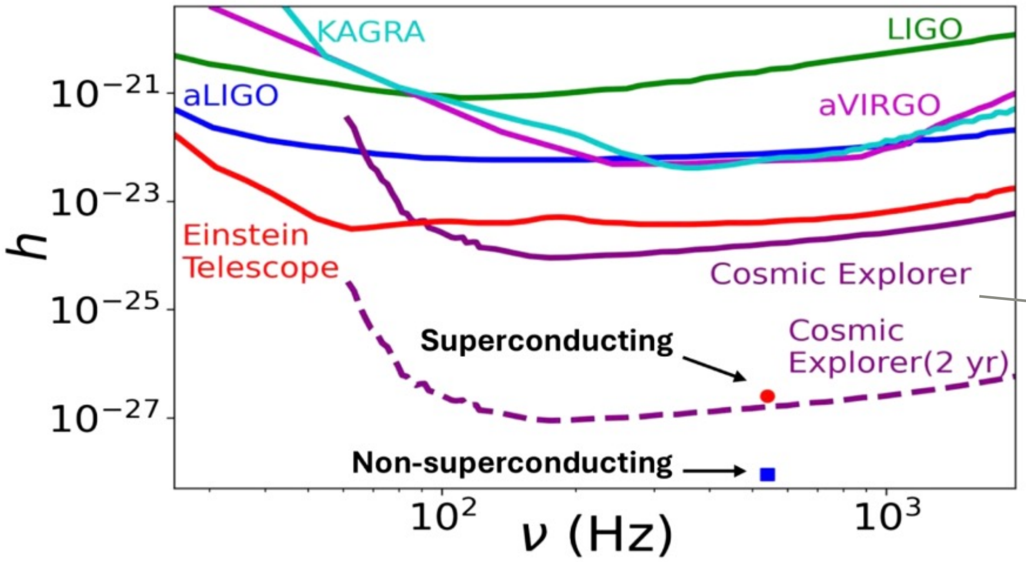

PHYSICAL REVIEW D **111,** L081307 (2025)

Letter

Superconductivity in magnetars: Exploring type-I and type-II states in toroidal magnetic fields

Mayusree Das,[1,*] Armen Sedrakian,[2,3,†] and Banibrata Mukhopadhyay[4,1,‡]

[1]*Joint Astronomy Programme, Department of Physics, Indian Institute of Science, Bangalore 560012, India*

[2]*Frankfurt Institute for Advanced Studies, D-60438 Frankfurt am Main, Germany*

[3]*Institute of Theoretical Physics, University of Wroclaw, 50-204 Wroclaw, Poland*

[4]*Department of Physics, Indian Institute of Science, Bangalore 560012, India*

(Received 26 January 2025; accepted 3 April 2025; published 30 April 2025)

We present a first two-dimensional general relativistic analysis of superconducting regions in axially symmetric highly magnetized neutron star (magnetar) models with toroidal magnetic fields. We investigate the topology and distribution of type-II and type-I superconducting regions for varying toroidal magnetic field strengths and stellar masses by solving the Einstein-Maxwell equations using the XNS code. Our results reveal that the outer cores of low- to intermediate-mass magnetars sustain superconductivity over larger regions compared to higher-mass stars with nontrivial distribution of type-II and type-I regions. Consistent with previous one-dimensional (1D) models, we find that regardless of the gravitational mass, the inner cores of magnetars with toroidal magnetic fields are devoid of *S*-wave proton superconductivity. Furthermore, these models contain nonsuperconducting, torus-shaped regions; a novel feature absent in previous 1D studies. Finally, we speculate on the potential indirect effects of superconductivity on continuous gravitational wave emissions from millisecond pulsars, such as PSR J1843-1113, highlighting their relevance for future gravitational wave detectors.

DOI: 10.1103/PhysRevD.111.L081307

Profile 1 - like

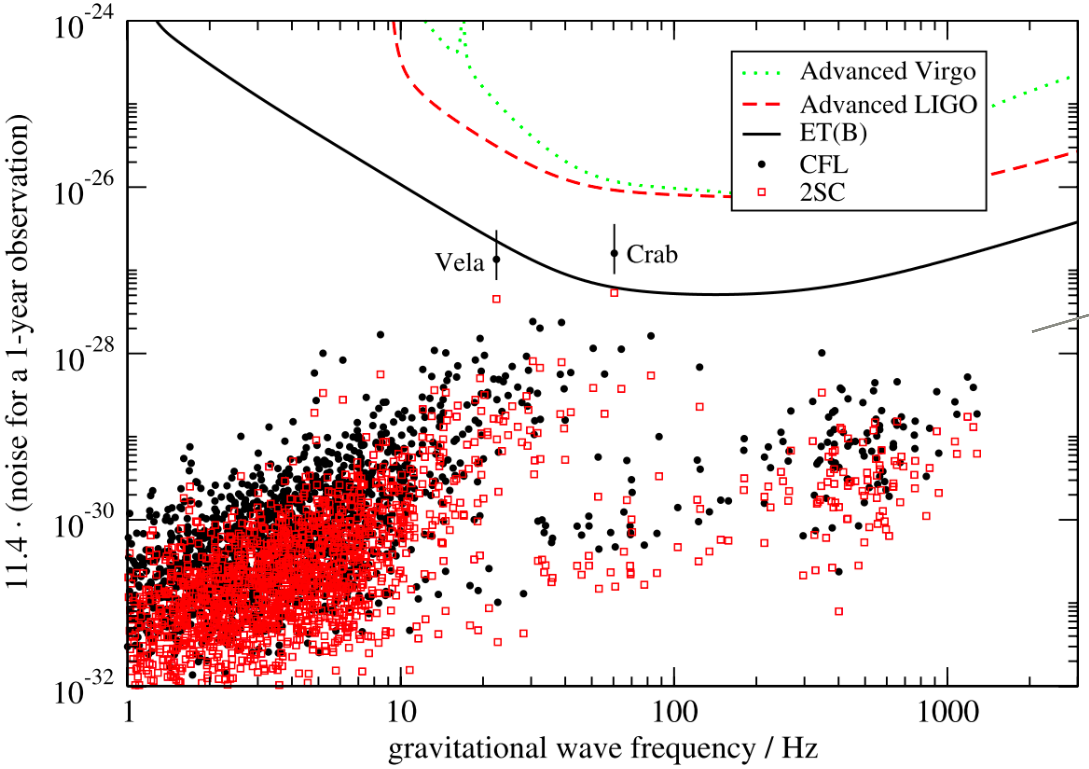

PRL **109,** 081103 (2012) PHYSICAL REVIEW LETTERS week ending 24 AUGUST 2012

Gravitational Waves from Color-Magnetic "Mountains" in Neutron Stars

K. Glampedakis,[1,2] D. I. Jones,[3] and L. Samuelsson[4,5]

[1]*Departamento de Física, Universidad de Murcia, E-30100 Murcia, Spain*

[2]*Theoretical Astrophysics, University of Tübingen, D-72076 Tübingen, Germany*

[3]*School of Mathematics, University of Southampton, Southampton SO17 1BJ, United Kingdom*

[4]*Department of Physics, Umeå University, SE-901 87 Umeå, Sweden*

[5]*Nordita, Roslagstullsbacken 23, SE-106 91 Stockholm, Sweden*

(Received 17 April 2012; published 22 August 2012)

Neutron stars may harbor the true ground state of matter in the form of strange quark matter. If present, this type of matter is expected to be a color superconductor, a consequence of quark pairing with respect to the color and flavor degrees of freedom. The stellar magnetic field threading the quark core becomes a color-magnetic admixture and, in the event that superconductivity is of type II, leads to the formation of color-magnetic vortices. In this Letter, we show that the volume-averaged color-magnetic vortex tension force should naturally lead to a significant degree of nonaxisymmetry in systems such as radio pulsars. We show that gravitational radiation from such color-magnetic "mountains" in young pulsars, such as the Crab and Vela, could be observable by the future Einstein Telescope, thus, becoming a probe of paired quark matter in neutron stars. The detectability threshold can be pushed up toward the sensitivity level of Advanced LIGO if we invoke an interior magnetic field about a factor ten stronger than the surface polar field.

DOI: 10.1103/PhysRevLett.109.081103 PACS numbers: 26.60.−c, 04.30.Tv, 12.38.−t, 97.60.Jd

Profile 2 - like

QUARK EoS & PARAMETERS

vBag model

Klähn & Fischer, ApJ (2015)

$$\mu_f = \mu_f^* + K_v n_f(\mu_f^*) \ , \tag{22}$$

$$P_f(\mu_f) = P_{FG,f}^{kin}(\mu_f^*) + \frac{K_v}{2} n_f^2(\mu_f^*) - B_\chi^f \ , \tag{23}$$

$$\varepsilon_f(\mu_f) = \varepsilon_{FG,f}^{kin}(\mu_f^*) + \frac{K_v}{2} n_f^2(\mu_f^*) + B_\chi^f \ , \tag{24}$$

$$n_f(\mu_f) = n_f(\mu_f^*). \tag{25}$$

$$\begin{aligned} \mu_u + \mu_e = \mu_d = \mu_s, \\ (2/3)n_u - (1/3)n_d - (1/3)n_s - n_e = 0. \end{aligned} \tag{2.5}$$

$$B_{\text{eff}} = \sum\nolimits_{f=u,d,s} B_{\chi,f} - B_{dc}.$$

(CFL) Color superconductivity

Lugones & Horvath, PRD (2002)

$$\Omega_{\text{CFL}} = \Omega_{\text{unpaired}} - (3/\pi^2)\Delta_{\text{SC}}^2\mu^2$$
$$P_{\text{CFL}} = P_{\text{unpaired}} + (3/\pi^2)\Delta_{\text{SC}}^2\mu^2$$
$$\epsilon_{\text{CFL}} = \epsilon_{\text{unpaired}} + (3/\pi^2)\Delta_{\text{SC}}^2\mu^2$$
$$n_{\text{CFL}} = n_{\text{unpaired}} + (2/\pi^2)\Delta_{\text{SC}}^2\mu^2$$

Quark parameters: B_{eff}, K_v and Δ_{CSC}

→ Determine extent of (color superconducting) quark core

QUARK CORE TRENDS

- Increase in B_{eff}
  → Point of PT shifts to higher densities
  → Decreases the extent of CSC matter in the star

Higher B_{eff} → higher energy cost to deconfine the quark phase → higher pressures/densities required for the stable quark phase to appear in the star.

- Increase in K_v
  → Point of PT shifts to higher densities
  → Decreases the extent of CSC matter in the star

Higher K_v → stiffer EoS in the quark phase (additional vector repulsion contribution). Pressure at a given μ reduces → require higher pressures for the PT.

- Increase in Δ_{CSC}
  → Point of PT shifts to lower densities
  → Increases the extent of CSC matter in the star

Higher Δ_{CSC} → pressure and energy density enhanced by the pairing energy $\sim \Delta_{\mathrm{CSC}}^2 \mu^2$ → point of PT reached at lower pressures

Star's magnetic field only affects the extent of *proton* superconductivity

Low field cases: $B_s = 10^{12}\ G, B_0 = 10^{15}\ G$

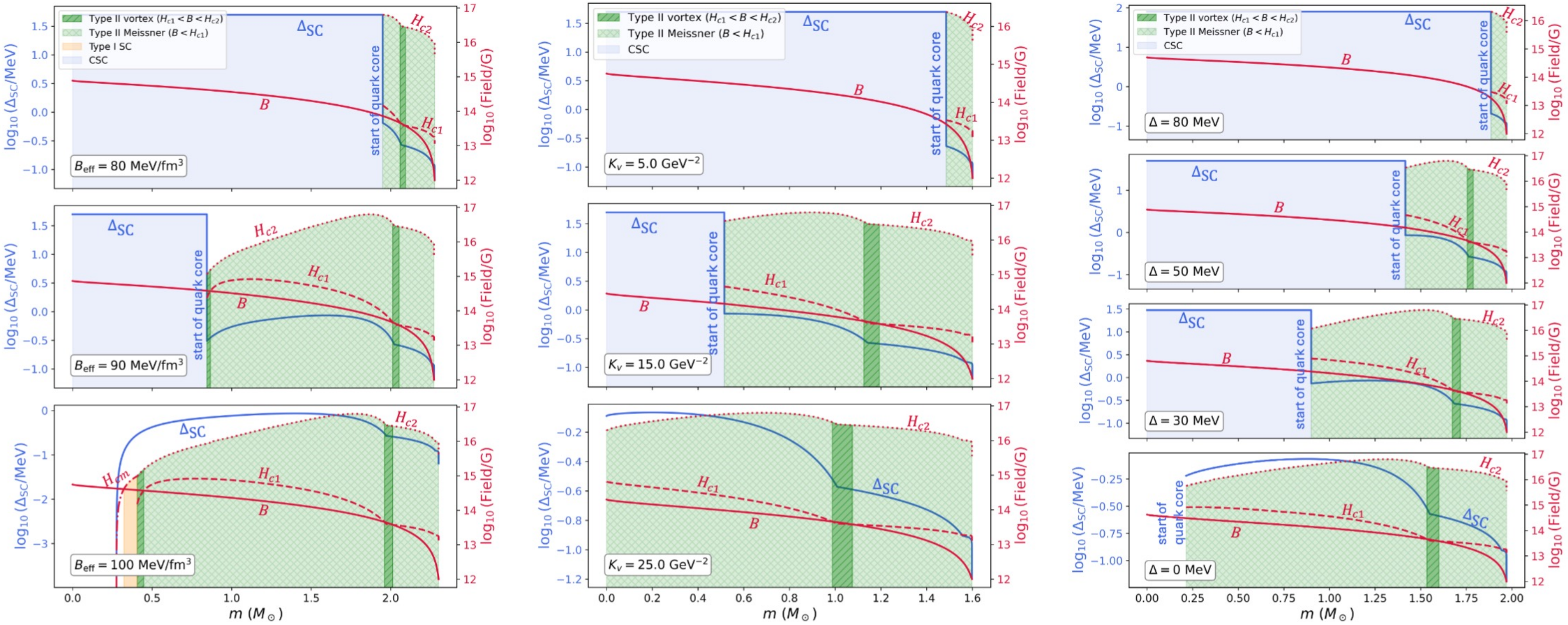

ENHANCED $M_{\max}$

Δ_{CSC} (MeV)	B_0 (G)	$B_{\mathrm{eff}} = 120$ MeV/fm^3			$B_{\mathrm{eff}} = 100$ MeV/fm^3			$B_{\mathrm{eff}} = 90$ MeV/fm^3			$B_{\mathrm{eff}} = 80$ MeV/fm^3		
		$M_{\max}(M_\odot)$	ϵ_c (MeV/fm^3)	$\epsilon_{\mathrm{trans}}$ (MeV/fm^3)	$M_{\max}(M_\odot)$	ϵ_c (MeV/fm^3)	$\epsilon_{\mathrm{trans}}$ (MeV/fm^3)	$M_{\max}(M_\odot)$	ϵ_c (MeV/fm^3)	$\epsilon_{\mathrm{trans}}$ (MeV/fm^3)	$M_{\max}(M_\odot)$	ϵ_c (MeV/fm^3)	$\epsilon_{\mathrm{trans}}$ (MeV/fm^3)
0	Isotropic	2.442	1055.33	1055.33	2.432	915.01	915.01	2.412	1027.27	825.42	2.369	956.02	706.51
	10^{15}	2.442	1055.33	1055.33	2.432	915.01	915.01	2.412	1027.27	825.42	2.369	956.02	706.51
	10^{18}	2.562	887.48	1055.33	2.562	887.48	915.01	2.558	825.42	825.42	2.518	822.05	706.51
10	Isotropic	2.442	1042.32	1042.32	2.43	906.36	906.36	2.408	1014.67	812.30	2.365	953.85	694.36
	10^{15}	2.442	1042.32	1042.32	2.43	906.36	906.36	2.408	1014.67	812.30	2.365	953.85	694.36
	10^{18}	2.562	887.48	1042.32	2.562	887.48	906.36	2.556	812.30	812.30	2.511	810.98	694.36
30	Isotropic	2.438	971.35	971.35	2.411	1030.94	818.85	2.368	943.25	712.62	2.302	1010.94	538.95
	10^{15}	2.438	971.35	971.35	2.411	1030.94	818.85	2.368	943.25	712.62	2.302	1010.94	538.95
	10^{18}	2.562	887.48	971.35	2.557	818.85	818.85	2.521	844.52	712.62	2.433	868.77	538.95
50	Isotropic	2.411	1070.35	825.42	2.295	640.97	640.97	2.253	1050.92	486.49	2.248	1131.53	245.04
	10^{15}	2.411	1070.35	825.42	2.295	640.97	640.97	2.253	1050.92	486.49	2.248	1131.53	245.04
	10^{18}	2.558	825.42	825.42	2.461	814.75	640.97	2.367	921.89	486.49	2.437	873.30	245.04
80	Isotropic	2.179	1046.44	505.88	2.151	1249.07	271.02	-	-	-	-	-	-
	10^{15}	2.179	1067.50	505.88	2.151	1249.07	271.02	-	-	-	-	-	-
	10^{18}	2.385	887.48	505.88	2.445	848.80	271.02	-	-	-	-	-	-
100	Isotropic	2.068	1374.99	294.37	-	-	-	-	-	-	-	-	-
	10^{15}	2.068	1374.99	294.37	-	-	-	-	-	-	-	-	-
	10^{18}	2.476	820.78	294.37	-	-	-	-	-	-	-	-	-

Profile 1

Δ_{CSC} (MeV)	B_0 (G)	$B_{\mathrm{eff}} = 120$ MeV/fm^3			$B_{\mathrm{eff}} = 100$ MeV/fm^3			$B_{\mathrm{eff}} = 90$ MeV/fm^3			$B_{\mathrm{eff}} = 80$ MeV/fm^3		
		$M_{\max}(M_\odot)$	ϵ_c (MeV/fm^3)	$\epsilon_{\mathrm{trans}}$ (MeV/fm^3)	$M_{\max}(M_\odot)$	ϵ_c (MeV/fm^3)	$\epsilon_{\mathrm{trans}}$ (MeV/fm^3)	$M_{\max}(M_\odot)$	ϵ_c (MeV/fm^3)	$\epsilon_{\mathrm{trans}}$ (MeV/fm^3)	$M_{\max}(M_\odot)$	ϵ_c (MeV/fm^3)	$\epsilon_{\mathrm{trans}}$ (MeV/fm^3)
0	Isotropic	2.442	1055.33	1055.33	2.432	915.01	915.01	2.412	1027.27	825.42	2.369	956.02	706.51
	10^{15}	2.442	1055.33	1055.33	2.432	915.01	915.01	2.412	1027.27	825.42	2.369	956.02	706.51
	10^{18}	2.562	887.48	1055.33	2.562	887.48	915.01	2.558	825.42	825.42	2.518	822.05	706.51
10	Isotropic	2.442	1042.32	1042.32	2.43	906.36	906.36	2.408	1014.67	812.30	2.365	953.85	694.36
	10^{15}	2.442	1042.32	1042.32	2.43	1142.17	906.36	2.408	1014.67	812.30	2.365	953.85	694.36
	10^{18}	2.562	887.48	1042.32	2.562	887.48	906.36	2.556	812.30	812.30	2.511	810.98	694.36
30	Isotropic	2.438	971.35	971.35	2.411	1030.94	818.85	2.368	943.25	712.62	2.302	1010.94	538.95
	10^{15}	2.438	971.35	971.35	2.411	1030.94	818.85	2.369	946.55	712.62	2.310	1000.59	538.95
	10^{18}	2.562	887.48	971.35	2.557	818.85	818.85	2.521	844.52	712.62	2.434	868.77	538.95
50	Isotropic	2.411	1070.35	825.42	2.295	640.97	640.97	2.253	1050.92	486.49	2.248	1131.53	245.04
	10^{15}	2.411	1066.85	825.42	2.325	935.14	640.97	2.282	1012.50	486.49	2.303	999.05	245.04
	10^{18}	2.558	825.42	825.42	2.470	795.44	640.97	2.414	870.67	486.49	2.455	841.94	245.04
80	Isotropic	2.179	1046.44	505.88	2.151	1249.07	271.02	-	-	-	-	-	-
	10^{15}	2.241	988.21	505.88	2.291	905.64	271.02	-	-	-	-	-	-
	10^{18}	2.396	862.63	505.88	2.492	770.84	271.02	-	-	-	-	-	-
100	Isotropic	2.068	1374.99	294.37	-	-	-	-	-	-	-	-	-
	10^{15}	2.291	811.82	294.37	-	-	-	-	-	-	-	-	-
	10^{18}	2.568	680.05	294.37	-	-	-	-	-	-	-	-	-

Profile 2

ENHANCED M_{max}

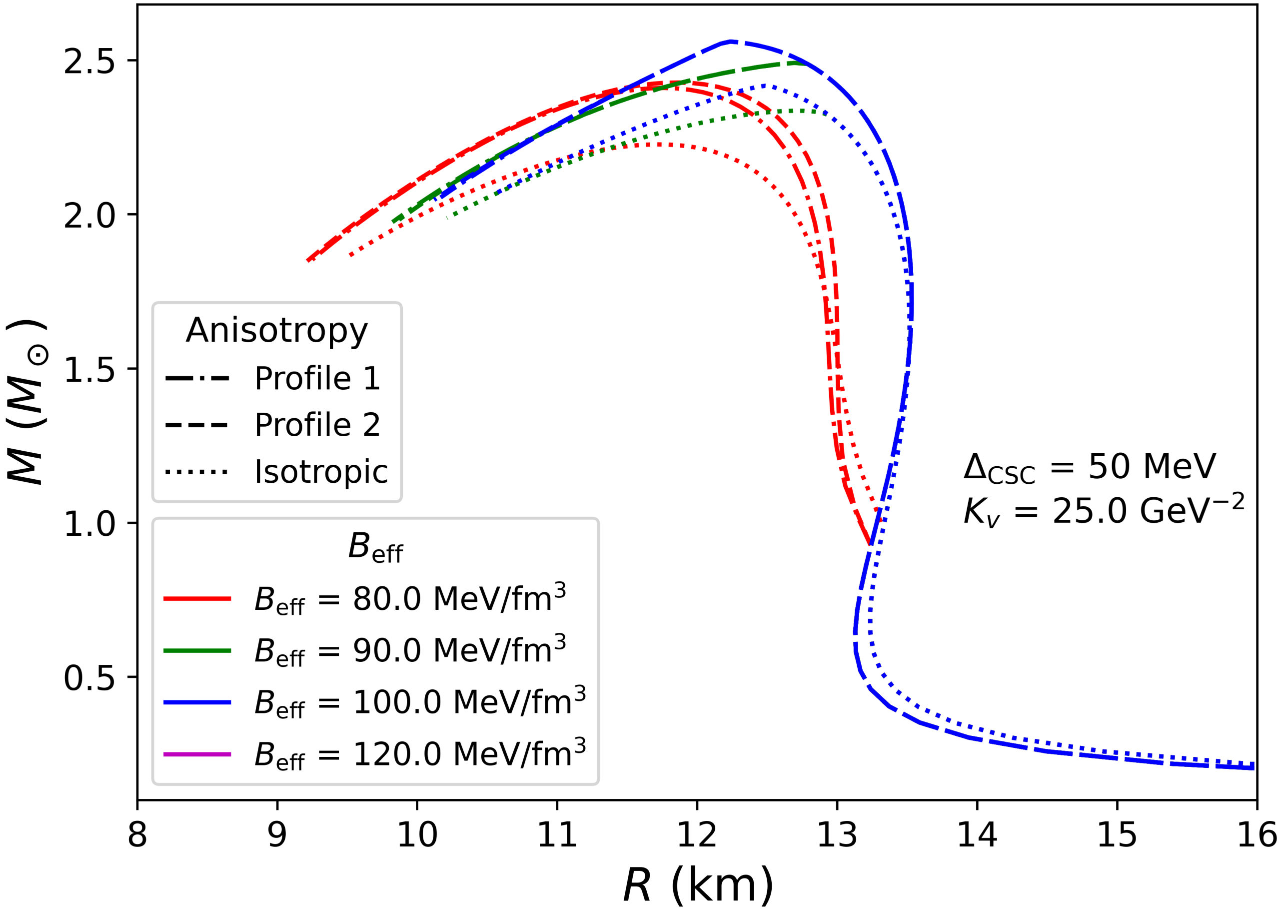

- When the PT leads to unstable branch → Role of magnetic field - enhances mass of hadron star before quark core forms
- Presence of CSC core leads to **CSC softening**: Compensated by anisotropy for $\Delta_{CSC} > 50$ MeV

Magnetic field profile:

$\eta = 0.01, \gamma = 1, B_s = 10^{15}\ G, B_0 = 10^{18}\ G$, TO

ENHANCED $M_{\max}$

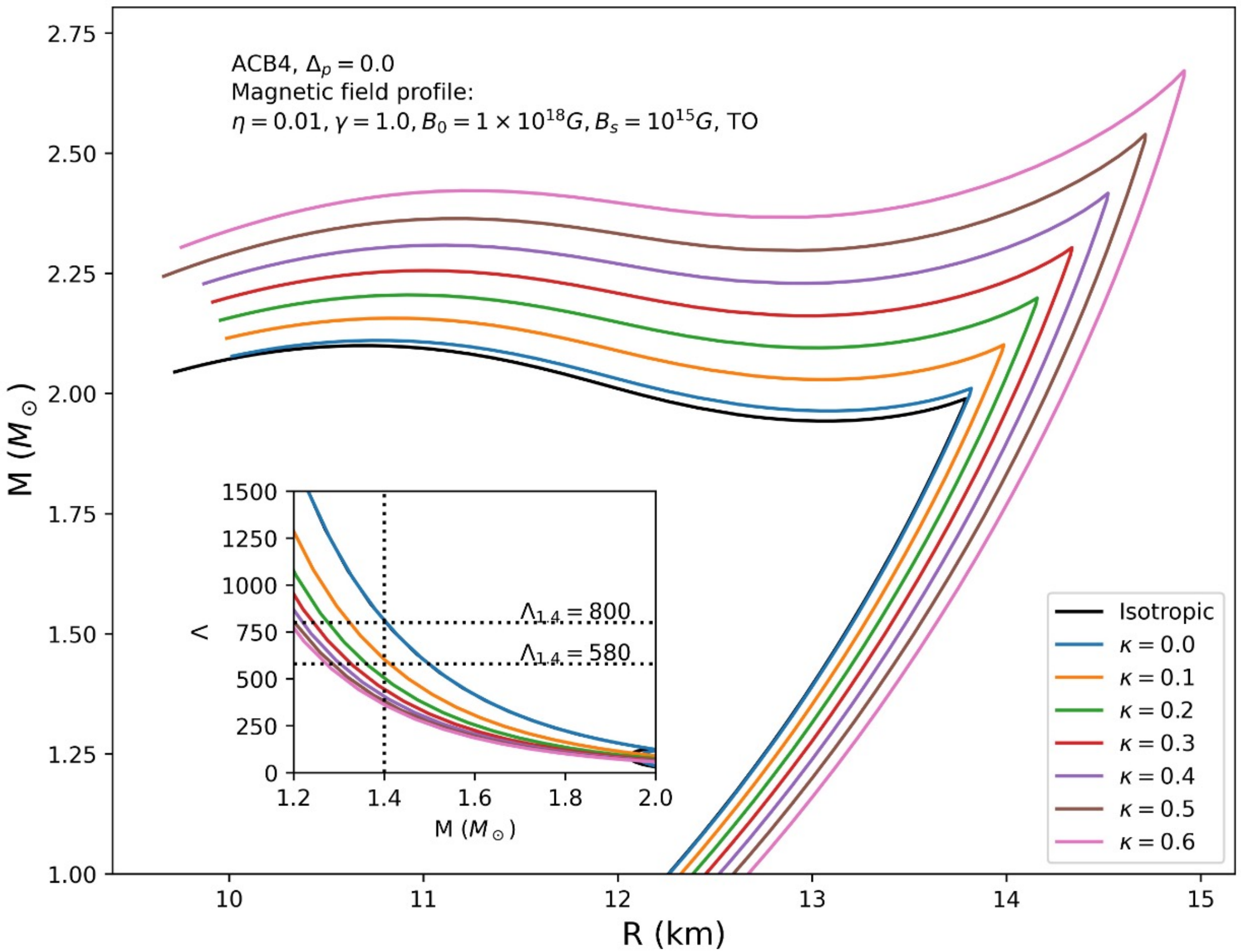

ZZ et al., Universe (2026)

We have recently shown similar mass enhancement of **hadronic branch** before PT due to **magnetic field** for different hybrid star set-up.

Hybrid star EoS: ACB4

Paschalidis et. al., PRD (2018)

Magnetic field profile:

$\eta = 0.01, \gamma = 1, B_s = 10^{15}\ G, B_0 = 10^{18}\ G$, TO

Anisotropy profile: Modified BL

Bowers & Liang, ApJ (1974)

Deb, Mukhopadhyay & Weber, ApJ (2021, 2022)